Exploration of the Feasibility of Polar Drive on the LMJ

Lindsay M. Mitchel

Spencerport High School

Spencerport, New York

Advisor: Dr. R. S. Craxton

Laboratory for Laser Energetics

University of Rochester

Rochester, NY

March 2010

Abstract

The Laser MegaJoule (LMJ), a laser system being constructed in France, is very similar to the U.S. National Ignition Facility (NIF) and is also designed to operate using an indirect drive configuration. However, it is desirable that the LMJ, like the NIF, have the capability to operate using direct drive, despite its less favorable geometry. Currently two types of direct drive experiments are planned for the NIF: initial implosions of hydrogen-filled glass targets with low energy (≤ 1.0 MJ) to produce neutrons to test diagnostics, and later implosions of cryogenic targets with higher energy (1.5 MJ) to obtain breakeven. These experiments employ a method known as polar drive in which beams are repointed toward the equator. The possibility of doing these experiments on the LMJ has been explored using the two-dimensional simulation code *SAGE*. Optimum designs for both experiments were created by adjusting parameters including the beam defocus distance and the beam pointings, and by using a new asymmetric beam shape. The levels of uniformity obtained are comparable to those expected for the NIF, proving that polar drive is feasible on the LMJ.

1. Introduction

Fusion is a nuclear reaction in which light nuclei of hydrogen combine, resulting in a heavier nucleus and a large release of energy. The light nuclei are isotopes of hydrogen and are called deuterium (D) and tritium (T). The deuterium nucleus has one proton and one neutron, and the tritium nucleus has one proton and two neutrons. Fusion of light nuclei can occur when lasers are shot at a capsule. Typically, the capsule is a spherical shell with a diameter of about 1 mm, is filled with hydrogen gas, and can be made from a variety of materials including plastic and glass. The laser bombardment causes the shell of the capsule to ablate outward. As a result, an equal and opposite force is applied to the inside of the capsule which implodes or compresses the

hydrogen to high temperatures, pressures, and densities. These conditions enable the hydrogen nuclei to overcome electrostatic forces (repellent forces between the positively charged nuclei) and fuse into a helium nucleus. This nucleus is responsible for 20% of the fusion energy. This energy can be deposited into the compressed hydrogen, initiating further fusion reactions in a self-sustaining chain reaction, a process called ignition. Ignition is obtained when there is a sufficient thickness of compressed hydrogen, which requires a laser with sufficient energy. A consequence of ignition is break-even. Break-even is when the energy output is equivalent to the energy input. The energy released from the fusion reactions could potentially satisfy the world's energy needs indefinitely. In order to reach these goals a capsule must be imploded uniformly.

Two methods are being explored to obtain the uniform implosion of a capsule. The first is direct drive,[1] in which the laser beams are pointed uniformly from all directions toward the center of the capsule, as illustrated in Figure 1a. The second method is indirect drive,[2] illustrated in Figure 1b. The indirect drive target is made of a hohlraum and a spherical capsule. The hohlraum is a cylinder (usually gold in material) and is similar in shape to a soda can with holes at both ends. The laser beams enter the holes and are absorbed by the walls of the hohlraum. The hohlraum walls release x rays, which bombard and uniformly implode the capsule located in the center of the hohlraum.

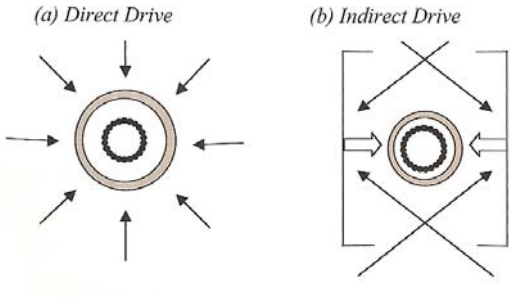

Figure 1. (a) In direct drive beams are uniformly pointed at the center of the capsule from all directions. (b) In indirect drive the beams enter the holes of the hohlraum and are absorbed by its walls. The walls release x rays which bombard and implode the capsule.

The U.S. National Ignition Facility (NIF) is a 192-beam laser fusion facility, designed with sufficient energy to achieve ignition and a consequent energy output 10 times greater than

the energy input. The NIF is designed for indirect drive using a hohlraum with a vertically oriented axis. The beams of the NIF are arranged into four rings in each of the upper and lower hemispheres, with angles θ of 23º to 50º from the axis, in order to enter the hohlraum holes. It is desirable that the NIF have the capability to operate using direct drive. Direct drive is a convenient way of producing neutrons necessary to test diagnostics. Also, direct drive presents a possible alternative method of achieving ignition and breakeven. However, due to the NIF beam configuration, if the beams are pointed at the center of the capsule there will be a lack of absorbed laser energy near the equator of the capsule, leading to a subsequent lack of drive or implosion in this area and an imploding shell that is elliptical rather than spherical (see Figure 2a). To compensate for this problem the laser beams can be repointed away from the center of the capsule, toward the equator, in a method known as polar drive[3] (see Figure 2b). Designs exist which prove that polar drive is a feasible method for uniform target implosion on the NIF[3-7].

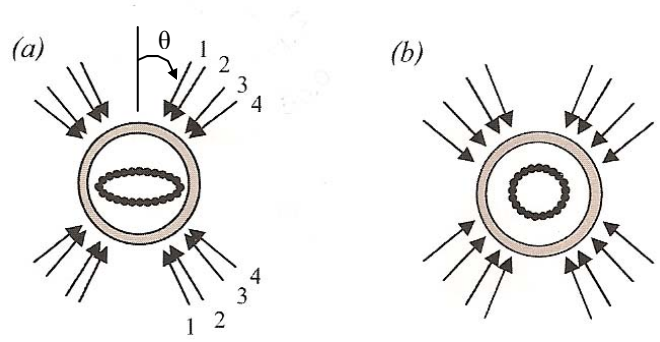

Figure 2. (a) If the NIF beams are pointed at the center of the capsule in direct drive there is a subsequent lack of drive at the equator due to the indirect drive beam configuration. (b) In direct drive the beams can be repointed away from the capsule's center, toward the equator, augmenting the implosion in this area.

The Laser MegaJoule (LMJ) is a 160-beam laser facility that is being constructed in Bordeaux, France and will have an indirect drive configuration, similar to the NIF. The LMJ will only have two rings of beams in each hemisphere, at angles of 33.2º and 49.0º from the axis. This makes the LMJ beam configuration less favorable than the NIF for direct drive and makes obtaining direct-drive uniformity a challenge. This work explored whether the beams of the LMJ

could be adjusted in order to obtain uniform direct-drive target implosions equivalent to the existing NIF designs.

Different parameters of the laser beams were adjusted including beam shape, defocus distance, and pointings. Designs were tested for experiments with two different types of targets: a spherical DT gas-filled glass (SiO_2) capsule with low energy (350 kJ) and a larger spherical cryogenic capsule with high energy (1.5 MJ). The glass capsule has a diameter of 0.15 cm. The gas density is $2.08X10^{-3}$ g/cm^3 corresponding to 10 atm of DT. For the glass capsule the laser pulse used has a Gaussian profile as seen in Figure 3. The pulse reaches its peak at 2.5 ns and continues for 5.0 ns. Experiments using the glass target would test neutron diagnostics. The cryogenic capsule has a layer of frozen DT inside a thin plastic (CH) shell and is driven by the shaped laser pulse shown in Figure 3(b). The outer diameter of the cryogenic capsule is 0.338 cm and the inner diameter is 0.27 cm. The density of the frozen DT layer is 0.25 g/cm^3 and there is some DT gas inside the frozen layer with density $1.58X10^{-5}$ g/cm^3. Experiments using the cryogenic target would obtain breakeven. It was found that the LMJ will be able to produce uniform target implosions equivalent to those of the NIF.

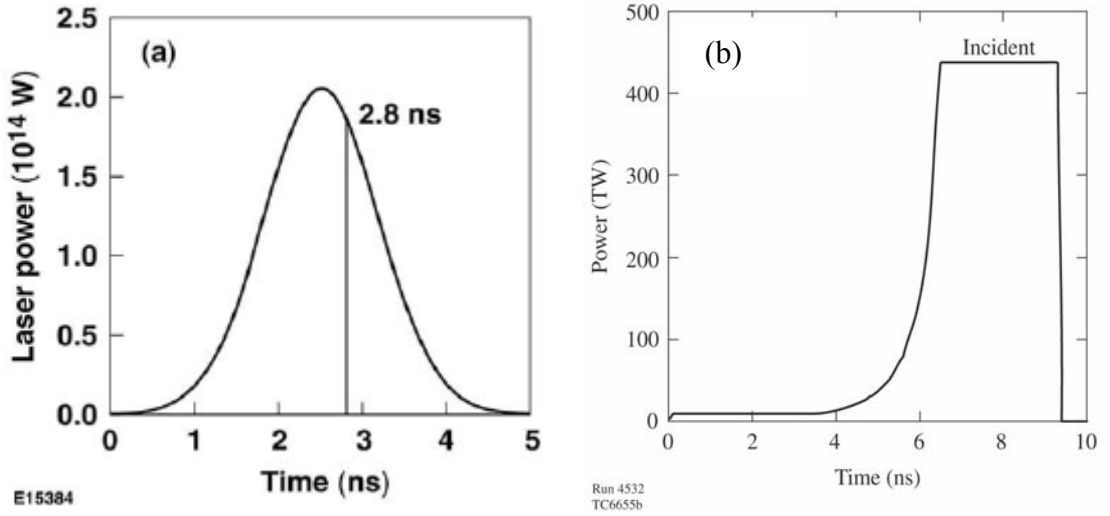

Figure 3. (a) Laser power as a function of time (ns) for the Gaussian laser pulse used on the glass target. At 2.8 ns, the glass shell has imploded to half its initial radius. [From Ref. 6] (b) Laser power as a function of time for the cryogenic target. [From Ref. 5]

2. Optimized Parameters

The first step to overcoming the unfavorable geometry of the LMJ and creating the optimum designs was to divide the first ring of beams at 33.2º into two separate rings.[8] Each ring contains 10 quads, a quad being a group of four beams that enter the target chamber through a single port and are generally focused on the same area. Every other quad was shifted toward the upper pole for ring 1, while the other quads at 33.2º were shifted toward the equator, creating ring 2. Several parameters were adjusted or optimized in order to establish the optimum designs. The beam pointings were optimized for both target types. The beam pointings determine the location on the target where the beam will land. The beams are shifted through the tilting of an optics mirror (see Figure 4a). The pointings are measured by the distance shifted from the center of the target perpendicular to the original direction of the beam, as shown in Figure 4b. In addition, various parameters were optimized depending on the phase plate that will be available for each target. A phase plate is a piece of glass that is part of the optics each laser beam passes through (see Figure 4a). The phase plate can determine the size and shape of the beam spot as well as the intensity within the beam spot.

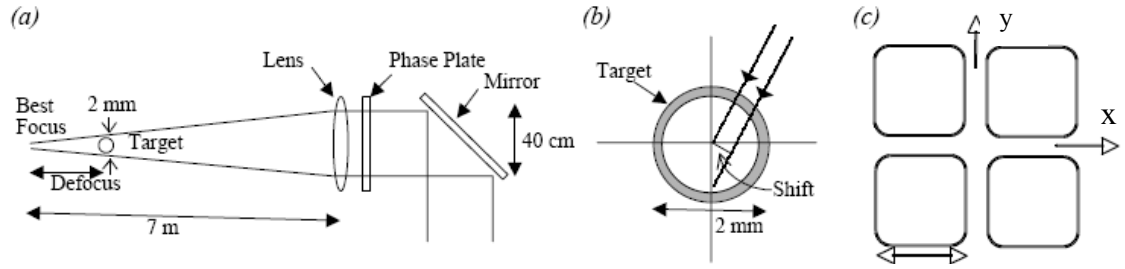

Figure 4. (a) The final optics that each beam will pass through. A beam can be repointed by tilting the mirror. A beam passes through the glass phase plate which determines the size, shape, and intensity of the beam spot. Also within the optics, changing the distance of the lens changes the focus of the beam spot. (b) When a beam is repointed, away from the center of the capsule, the distance of the beam shift is measured perpendicular to the original direction of the beam. (c) Four laser beams are grouped into a quad. To adjust the beam spot a quad can be split, by moving each beam in either the X or Y direction. [From Ref. 6]

2.1 Optimized Parameters for the Glass Target

For the glass target, it is assumed that the LMJ will have indirect drive phase plates similar to those on the NIF. These phase plates create small elliptical beam spots necessary for the beams to enter the hohlraum holes. However, for direct drive it is desirable to have larger beam spots that correspond to the size of the capsule. The grouping of the laser beams into quads on both the NIF and the LMJ is shown in Figure 4(c). Through the application of split quads each beam in a quad can be shifted in the X or Y direction to create a larger beam spot. The distance that each beam is shifted within the quad also affects the overall shape of the beam spot generated by the quad, as well as the intensity contours within the beam spot. In addition, the optics lens can be moved closer to the target along the line of the beam, as shown in Figure 4a. This results in the defocusing of the beam and creates a larger spot size of lower intensity. Through the use of split quads and defocusing, the beam spot size and intensity can be adjusted in order for the beams to blend together and provide uniform drive upon all areas of the target.

2.2 Optimized Parameters for the Cryogenic Target

For the cryogenic target it was assumed that custom phase plates would be available. Therefore, optimum phase plates were designed by optimizing the shape, size, and intensity of different beam rings. For each beam ring the intensity I is given as a function of radius r by the equation

$$I(r) = I_0 \exp\left[-(r/r_0)^n \right] \qquad (1)$$

where n is the Gaussian order, which is responsible for the shape of the intensity profile within the beam, r_0 is the radius of the beam spot, and I_0 is the maximum intensity in the beam. Two additional parameters for each beam are the intensity cutoff and the elliptical θ_e. The intensity cutoff is a specific intensity value at which the beam spot ends, defined as a percentage of I_0. The

elliptical θ_e is an angle which determines the ellipticity of the beam shape. This parameter can be understood as the beam spot being compressed in the vertical direction so that the intensity contours become ellipses. The ratio of the major (a) and minor (b) axes is given by a **:** b = $1/\cos\theta_e$ **:** 1.

However, an improved design was created using a new asymmetrical beam shape. The beam shape follows the Super Gaussian equation

$$I(r,\theta) = I_0 \exp [-(r/r_0(\theta))^{n(\theta)}] \quad (2)$$

which determines the intensity of the beam as a function of the angle θ. Here,

$$r_0(\theta) = r_{01} + r_{02} \cos\theta \quad (3)$$

$$n(\theta) = n_1 + n_2 \cos\theta \quad (4)$$

where r_{01} = 1200 μm, r_{02} = 200 μm, n_1 = 2.5 and n_2 = 0.5 in the design. For example, Figure 5 shows the beam spot used for ring 3 beams in (a) the symmetrical and (b) the asymmetrical cryogenic designs. In the symmetrical design n = 2.5 and r_0 = 1200 μm. In the asymmetrical design, n = 2.0 and r_0 = 1400 μm at the top of the beam, and n = 3.0 and r_0 = 1000 μm at the bottom. The intensity cutoff also had angle-dependent values. In addition the beam spot could be made elliptical similar to the symmetrical beam shape. The angle θ_e was 60° for the symmetrical beam spot and 55° for the asymmetrical beam spot.

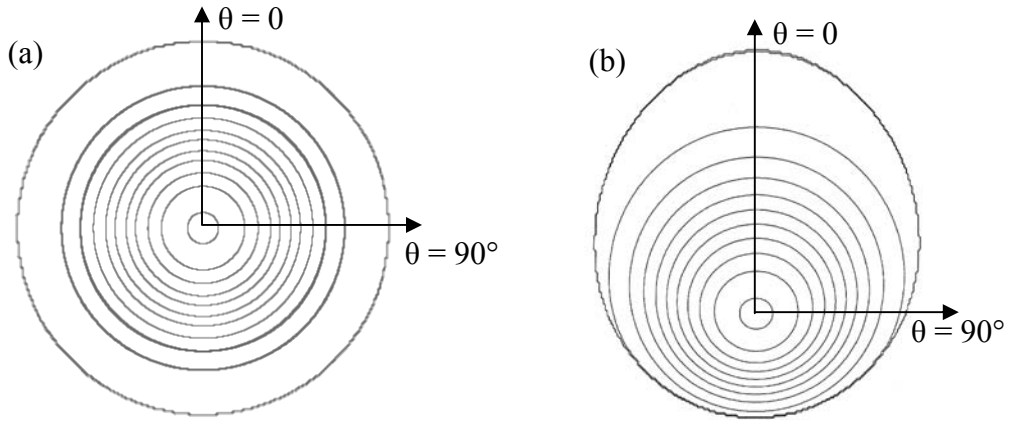

Figure 5. (a) Intensity contours (at 10% intervals) of a symmetrical beam shape with n =2.5 and r_0 = 1200 μm. (b) Intensity contours of an asymmetrical beam shape that has parameter values that differ as a function of angle. The beam spot developed for ring 3 beams has a gradual decrease in intensity at the upper pole and a steeper decrease in intensity at the lower pole. This shape provides extra drive at the equator and allows for a greater absorption of laser energy.

Using the asymmetrical beam shape provides two distinct advantages. First, the asymmetrical beam shape has a more intense bottom half that provides extra drive needed at the equator, while the upper half has a gradual decrease in intensity which allows for the ring 3 beams to blend easily with the other rings. The second advantage of the asymmetrical beam shape is that the bottom half is more compact with a smaller radius so that less energy is lost due to laser rays passing by the imploding target.

3. Optimization Process and, Optimized Designs

The two-dimensional hydrodynamics simulation code *SAGE*[9] was used to test a variety of designs for these targets.

3.1 Glass Target Optimum Design

Table 1. Parameter values for the glass target optimum design using indirect drive phase plates.

	Angle	Beam Pointings	Defocus Distance	Split Quad Y Shift (vertical)	Split Quad X Shift (horizontal)
Ring 1	33.2º	300 μm	2.625 cm	----	----
Ring 2	33.2º	-700 μm	2.625 cm	----	----
Ring 3	49.0º	-700 μm	2.625 cm	400 μm	200 μm

Table 1 gives the specific parameter values for the glass target optimum design. In Figure 6, ray trace plots show the rays of an incoming ring 3 beam and the density contours of imploding shells for both the NIF and LMJ glass target optimum designs. As the capsules implode they maintain their spherical shape through 2.8 ns. It is essential for uniformity to be consistent at 2.8 ns, at which time the majority of the laser energy has been deposited. Peak compression occurs slightly later, just after 3.0 ns. The small deviations from uniformity seen in

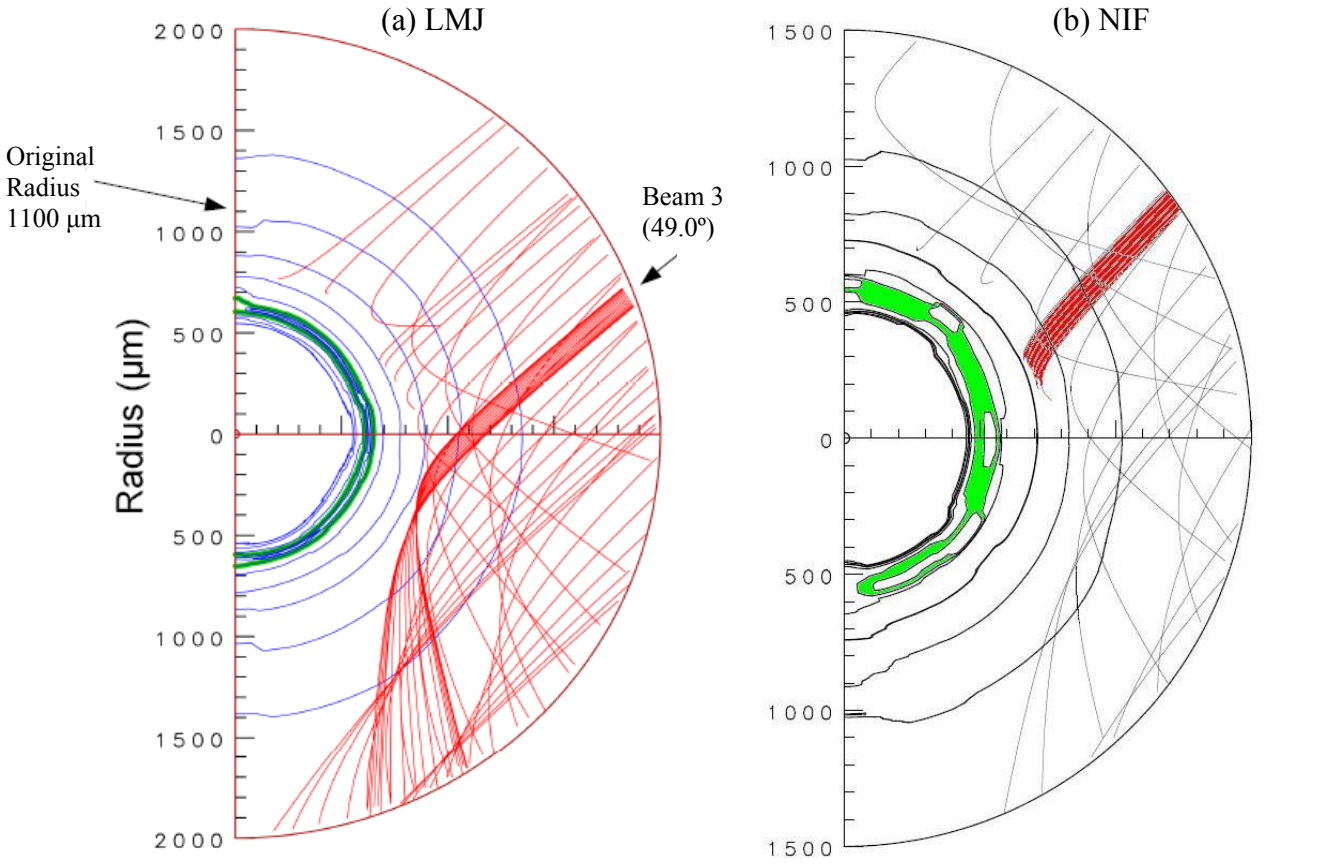

Figure 6. Ray trace plots generated by SAGE *which display the rays (primarily red) and the density contours (blue and black) of the imploded glass capsules (green) at 2.8 ns. The green areas represent regions where the density is above four times the critical density. Laser beams can not penetrate beyond the critical density. (a) LMJ optimum design. (b) NIF design. Both (a) and (b) show that the capsules have maintained their spherical shape and imploded uniformly.*

Figure 6 are shown more clearly in Figure 7, which gives the center-of-mass radius as a function of θ, the angle from the vertical axis, for the LMJ and NIF designs. Both graphs are relatively flat lines, indicating uniform drive at all angles. The LMJ design yielded an implosion with a low root mean square deviation of radius (ΔR_{rms}) of 5.2 µm, while the NIF design obtained a ΔR_{rms} of 6.5 µm at 2.8 ns. In addition, the velocity deviation was low; velocity uniformity was obtained within 2.5% for the LMJ design, which is comparable to the NIF design which obtained velocity uniformity within 1.7%.[6]

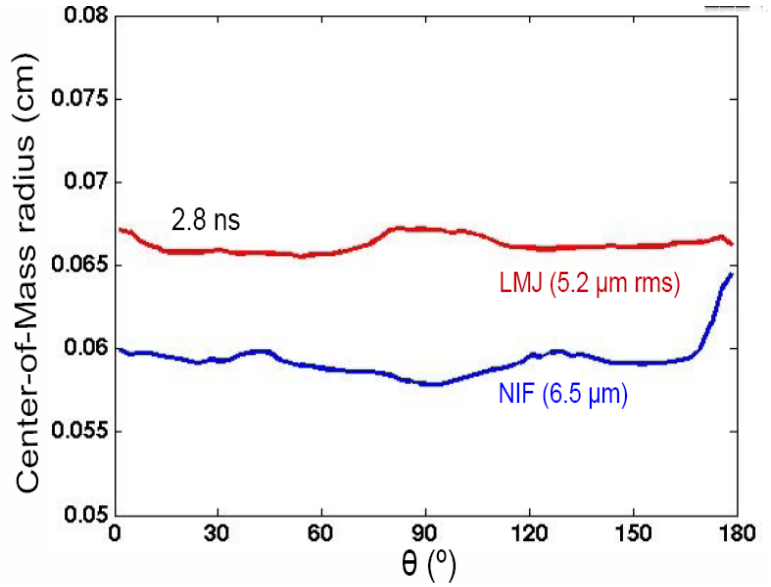

Figure 7. Center-of-mass radius of the imploding shell as a function of the angle θ from the vertical for both the LMJ and NIF glass target designs at 2.8 ns. The relatively flat lines represent the uniformity of the implosions at all angles.

The optimization process involved analyzing the simulations, primarily using ray trace plots such as Figure 6, and plots of the center-of-mass radius and velocity such as Figure 7. The results were evaluated at specific times, and promising runs had a low ΔR_{rms} and a low velocity deviation throughout the implosion. When a promising run was produced, specific parameter adjustments were more deeply explored in additional runs.

3.2 Optimum Cryogenic Design using Symmetrical Phase Plates

Table 2. Parameter values for the optimum cryogenic design using symmetric phase plates.

	Angle	Beam Pointings	Elliptical θ_e	Gaussian Order n	Radius R_0	Intensity Cutoff
Ring 1	33.2º	350 μm	----	2.5	1200 μm	1.0%
Ring 2	33.2º	-350 μm	50.0º	2.5	1200 μm	1.0%
Ring 3	49.0º	-800 μm	55.0º	2.5	1200 μm	1.0%

Table 2 gives the specific parameter values for the symmetrical cryogenic target optimum design. The ray trace plots in Figure 8 show a comparison between the shape of the LMJ and NIF capsules at 9.0 ns. In Figure 9 graphs of the center-of-mass radius as a function of θ

compare the implosion patterns of the LMJ and NIF designs at 9.0 ns. Both capsules preserved their spherical shape with the exception of slight protrusions at the equator, where there is a lack of drive. However, both capsules have imploded about 800 μm, half the original radius (1600 μm). The LMJ design obtained a ΔR_{rms} of 12.4 μm, while the NIF design obtained a ΔR_{rms} of 11.4 μm. In addition, velocity uniformity for the LMJ design was obtained within 2.6%, which is comparable to the NIF design that obtained velocity uniformity within 2.7%.

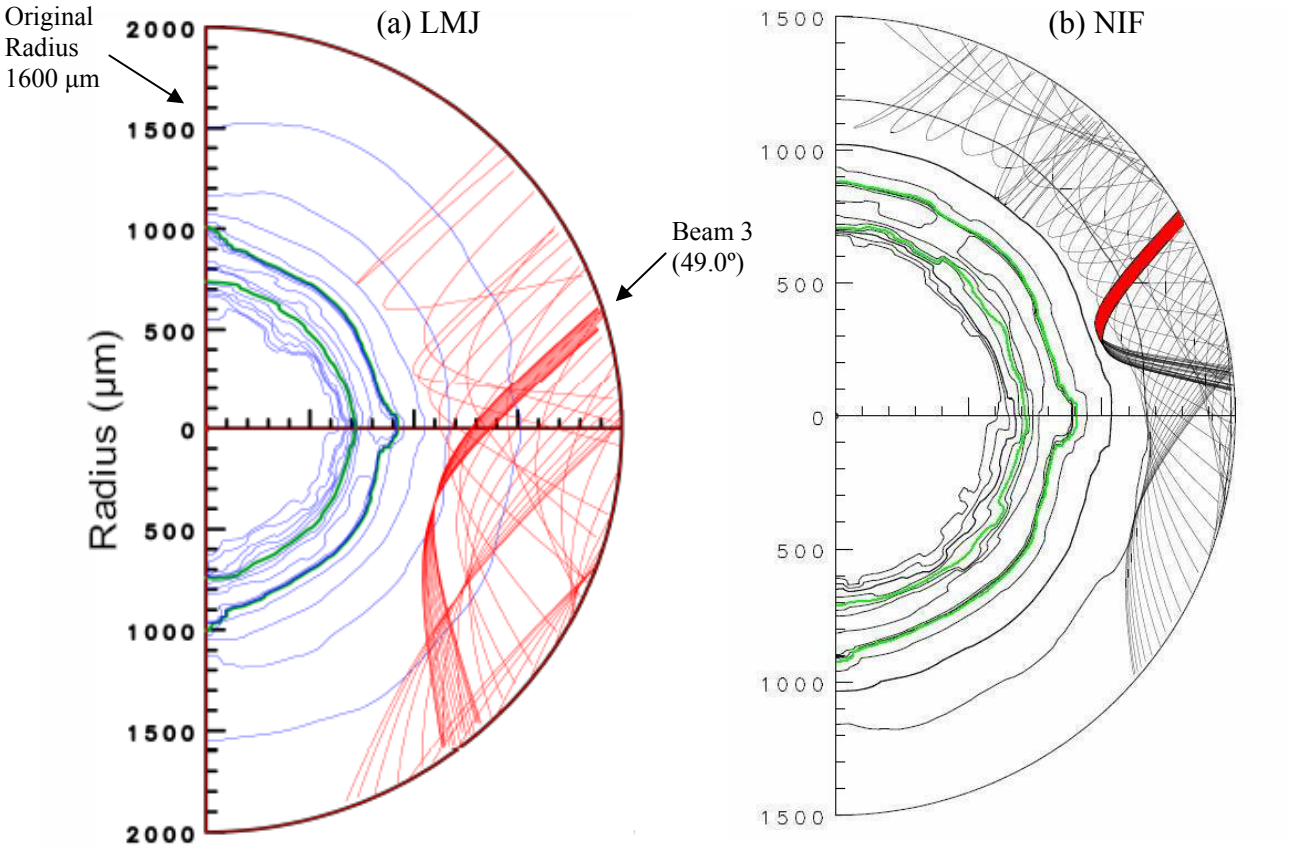

Figure 8. Ray trace plots generated by SAGE *which display the rays (primarily red) and the density contours (blue and black) of the imploded cryogenic capsules (green) at 9.0 ns. (a) LMJ optimum design; (b) NIF design. Both (a) and (b) illustrate that the capsules have preserved their spherical shape until the end of the laser pulse.*

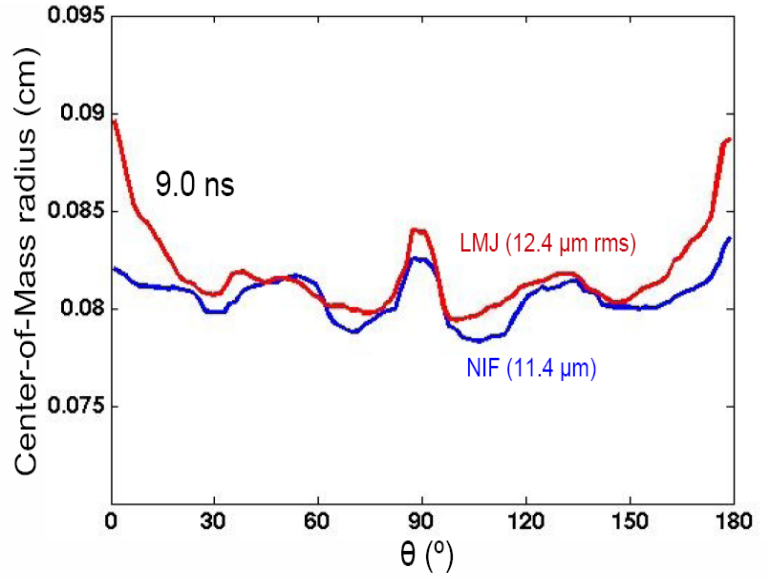

Figure 9. Center-of-mass radius of the imploding shell as a function of θ for both the LMJ and NIF cryogenic designs at 9.0 ns. Both implosion patterns show a lack of drive at the equator.

3.3 Cryogenic Design using Asymmetrical Phase Plates

Table 3. Parameter values for the optimum cryogenic design using asymmetrical phase plates.

	Angle	Beam Pointings	Elliptical θ_e	Gaussian Order n	Radius R_0	Intensity Cutoff	
Ring 1	33.2º	200 μm	30.0º	2.5	1200 μm	1.0%	
Ring 2	33.2º	-350 μm	40.0º	2.5	1200 μm	1.0%	
Ring 3	49.0º	-800 μm	60.0º	2.0	1400 μm	1.0%	Upper Pole θ=0.0º
				3.0	1000 μm	15.0%	Lower Pole θ=180.0º

Table 3 gives the specific parameter values for the second cryogenic design which employs the asymmetrical beam shape in Figure 5b for ring 3 (49.0º). This beam shape was developed in an attempt to reduce the protrusion at the equator of the symmetrical cryogenic design. The value of the asymmetrical beam shape can easily be seen in a comparison of the ray trace plots for the cryogenic design using asymmetrical phase plates (Figure 10) and the symmetrical optimum design (Figure 8a). The asymmetrical optimum design maintained its spherical shape through 9.0 ns, which is close to the end of the laser pulse. The ΔR_{rms} for the

asymmetrical design is 10.4 μm, which is more uniform than both the LMJ and NIF symmetrical designs.

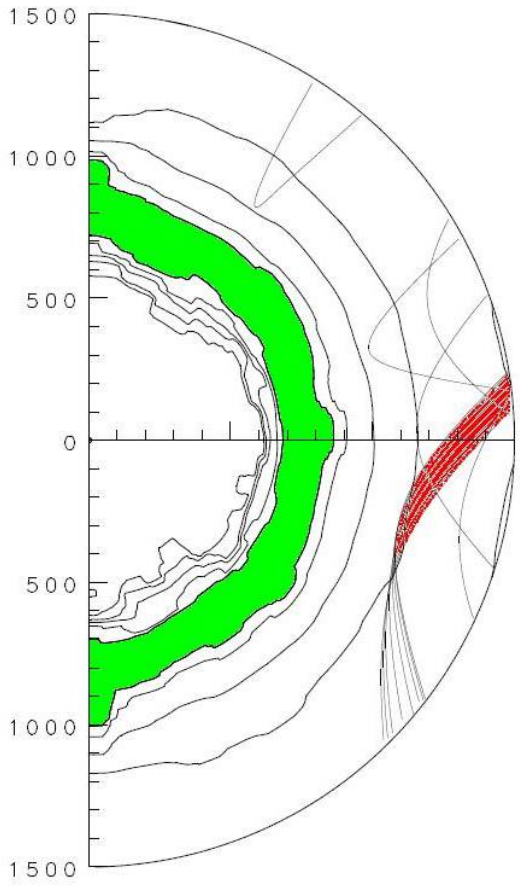

Figure 10. Ray trace plot generated by SAGE *which displays the rays (red) and the density contours (black) of the imploding capsule (green) for the cryogenic design using asymmetrical phase plates. The* ΔR_{rms} *for the implosion is 10.4 μm at 9.0 ns.*

The advantage of the asymmetrical beam shape is clearly seen in Figure 11, which plots the center-of-mass radius as a function of θ for the symmetrical and asymmetrical phase plates. The protrusion at the equator with the asymmetrical phase plates is less than that of the symmetrical design. The asymmetrical beam shape has increased the impact of ring 3 beams at the equator and alleviated the problem posed by the unfavorable geometry of the LMJ. In addition, the LMJ asymmetrical design obtained velocity uniformity within 2.2%, which is comparable to the LMJ symmetrical design which obtained velocity uniformity within 2.6%.

In addition, the asymmetrical beam shape allowed for a greater absorption of laser energy. For the symmetrical design absorption was 62% while for the asymmetrical design

absorption increased to 64%. As a result of the higher absorption, the asymmetrical design has a smaller center-of-mass radius than the symmetrical design, as seen in Figure 11.

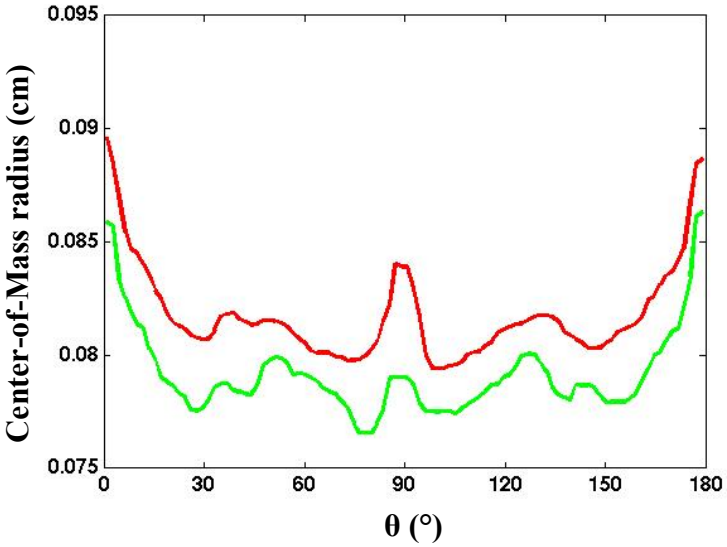

Figure 11. Center-of-mass radius of the imploded capsule as a function of θ for the LMJ design using symmetrical phase plates (red) and the LMJ design using asymmetrical phase plates (green).

Figures 8a, 10 and 11 show a weakness in drive at θ = 0 and θ = 180° for both the LMJ symmetrical and LMJ asymmetrical designs. These weak areas are most likely a result of the LMJ geometry, which has the first ring of beams at 33.2° in comparison to the NIF which has the first ring of beams at a lesser angle of 23.5°. This not a major problem because the solid angle affected is small. However, it is possible that the problem could be reduced through further optimization. One possible approach might be to point two beams out of each of the five quads of Ring 1 a little closer to the pole.

4. Conclusion

Three optimized polar drive designs have been developed for the LMJ laser facility. The designs are for two different types of targets: a spherical DT gas-filled glass capsule with low energy (350 kJ) and a larger spherical cryogenic DT capsule with high energy (1.5 MJ). The primary purpose of the gas-filled capsule is to produce high neutron yields necessary to test diagnostics. The second and third designs utilize the cryogenic capsule and allow for the

possibility of attaining ignition and breakeven. In particular, the third design uses an asymmetrical beam shape to enhance the uniformity of the implosion. The designs were optimized using hydrodynamic simulations to obtain levels of uniformity which are comparable to the uniformity of pre-existing NIF polar drive designs in spite of the unfavorable geometry of the LMJ. These designs show that the LMJ laser facility as well as the NIF will be compatible for both indirect drive and direct drive implosions.

5. Acknowledgments

I would like to thank my family for their encouragement throughout the program, and Jeremy P. Wyatt for his time and effort helping me prepare figures. Also, I would like to thank my advisor Dr. R. Stephen Craxton for his invaluable support and guidance. Finally, I am very grateful to Dr. Craxton and the Laboratory for Laser Energetics for giving me this extraordinary opportunity.

6. References

1. J. Nuckolls *et al*., "Laser Compression of Matter to Super-High Densities: Thermonuclear (CTR) Applications," Nature **239**, 139 (1972).
2. J. D. Lindl, "Development of the Indirect-Drive Approach to Inertial Confinement Fusion and the Target Basis for Ignition and Gain," Phys. Plasmas **2**, 3933 (1995).
3. S. Skupsky *et al*., "Polar Direct Drive on the National Ignition Facility." Phys. Plasmas **11**, 2763 (2004).
4. Alexandra M. Cok, "Development of Polar Direct Drive Designs for Initial NIF Targets," Laboratory for Laser Energetics High School Research Program (2006).
5. R. S. Craxton and D. W. Jacob-Perkins, "The Saturn Target for Polar Direct Drive on the National Ignition Facility," Phys. Rev. Lett. **94**, 095002 (2005).
6. A. M. Cok *et al*., "Polar-drive designs for optimizing neutron yields on the National Ignition Facility," Phys. Plasmas **15**, 082705 (2008).
7. R. S. Craxton et al., "Polar Direct Drive: Proof-of-Principle Experiments on OMEGA and Prospects for Ignition on the National Ignition Facility," Phys. Plasmas **12**, 056304 (2005).
8. R. S. Craxton, "Hydrodynamic Simulations of Polar Direct Drive on the NIF and LMJ Based on Three-Dimensional Ray Tracing," 45th Annual Meeting of the American Physical Society Division of Plasma Physics (2003).
9. R. S. Craxton and R. L. McCrory, "Hydrodynamics of Thermal Self-Focusing in Laser Plasmas," J. Appl. Physics. **56**, 108 (1984).